

# *C. elegans* mitochondrial factor WAH-1 promotes phosphatidylserine externalization in apoptotic cells through phospholipid scramblase SCRM-1

Xiaochen Wang<sup>1,5</sup>, Jin Wang<sup>2</sup>, Keiko Gengyo-Ando<sup>3</sup>, Lichuan Gu<sup>4</sup>, Chun-Ling Sun<sup>1</sup>, Chonglin Yang<sup>1</sup>, Yong Shi<sup>1</sup>, Tetsuo Kobayashi<sup>3</sup>, Yigong Shi<sup>4</sup>, Shohei Mitani<sup>3</sup>, Xiao-Song Xie<sup>2</sup> and Ding Xue<sup>1,6</sup>

**Externalization of phosphatidylserine, which is normally restricted to the inner leaflet of plasma membrane, is a hallmark of mammalian apoptosis<sup>1–4</sup>. It is not known what activates and mediates the phosphatidylserine externalization process in apoptotic cells. Here, we report the development of an annexin V-based phosphatidylserine labelling method and show that a majority of apoptotic germ cells in *Caenorhabditis elegans* have surface-exposed phosphatidylserine, indicating that phosphatidylserine externalization is a conserved apoptotic event in worms. Importantly, inactivation of the gene encoding either the *C. elegans* apoptosis-inducing factor (AIF) homologue (WAH-1)<sup>5</sup>, a mitochondrial apoptogenic factor, or the *C. elegans* phospholipid scramblase 1 (SCRM-1), a plasma membrane protein, reduces phosphatidylserine exposure on the surface of apoptotic germ cells and compromises cell-corpse engulfment. WAH-1 associates with SCRM-1 and activates its phospholipid scrambling activity *in vitro*. Thus WAH-1, after its release from mitochondria during apoptosis, promotes plasma membrane phosphatidylserine externalization through its downstream effector, SCRM-1.**

Although phosphatidylserine externalization is a widespread phenomenon in mammalian apoptosis<sup>1–4</sup>, it is unclear whether it occurs during apoptosis in other organisms. To examine whether phosphatidylserine is externalized in apoptotic cells in *C. elegans*, we developed a gentle surgical procedure to expose *C. elegans* gonads and then used fluorescence-conjugated annexin V, a highly specific phosphatidylserine-binding protein, to stain apoptotic germ cells that are on the surface of gonads<sup>6</sup>. When exposed gonads from *ced-1(e1735)* animals (which are defective in cell-corpse engulfment and thus allow assay of more germ-cell corpses<sup>7</sup>) were stained, 62% of germ-cell corpses were labelled with annexin V, resulting in bright ring-shaped staining (Fig. 1a, c). We confirmed that the

cells labelled with annexin V corresponded to apoptotic germ cells by their raised disc-like morphology under Nomarski optics and condensed Hoechst 33342 chromosomal DNA staining pattern, characteristic of apoptotic cells<sup>6</sup>. These phosphatidylserine-positive cells were not stained with propidium iodide and thus were not necrotic or damaged germ cells (data not shown). In addition, no annexin V staining was observed in exposed gonads of *ced-1(e1735); ced-3(n717)* animals (Fig. 1b), in which all germ-cell deaths were blocked by a *ced-3(n717)* loss-of-function mutation<sup>6</sup>, providing further confirmation that annexin V only stains apoptotic cells. A higher percentage of phosphatidylserine staining (84%) was observed in germ-cell corpses in *ced-2(n1994)* animals (Fig. 1c), which are also defective in cell-corpse engulfment<sup>7</sup>. In addition, animals of different adult ages had similar percentages of germ-cell corpses stained with annexin V (see Supplementary Information, Table S1).  $\gamma$ -irradiation was also used to induce apoptosis in the germline of wild-type animals and resulted in a similar percentage of germ-cell corpses (56%) with surface-exposed phosphatidylserine (Fig. 1d). These results indicate that phosphatidylserine is exposed on the surface of a significant portion of germ-cell corpses in *C. elegans*, and that phosphatidylserine externalization is a conserved apoptotic event in *C. elegans*.

This phosphatidylserine staining protocol was then used to search for regulatory factors and enzymes involved in promoting phosphatidylserine externalization during *C. elegans* apoptosis. It has been reported previously that microinjection or overexpression of human AIF in cultured cells can induce surface phosphatidylserine exposure<sup>8,9</sup>. However, it is unclear whether AIF has a direct causal effect on phosphatidylserine externalization. This possibility was examined by using RNA interference (RNAi) to reduce *C. elegans wah-1* expression and then staining for phosphatidylserine in *ced-1(e1735); wah-1(RNAi)* animals. Compared with 60% of germ-cell corpses stained in *ced-1(e1735); control(RNAi)* animals, only 22% of germ-cell corpses in *ced-1(e1735); wah-1(RNAi)* animals were labelled with annexin V (Fig. 1c). Similarly, *wah-1* RNAi

<sup>1</sup>Department of Molecular, Cellular, and Developmental Biology, University of Colorado, Boulder, CO 80309, USA. <sup>2</sup>McDermott Center for Human Growth and Development, University of Texas Southwestern Medical Center, Dallas, TX 75390, USA. <sup>3</sup>Department of Physiology, Tokyo Women's Medical University, School of Medicine, and CREST, JST, Tokyo, 162-8666, Japan. <sup>4</sup>Department of Molecular Biology, Princeton University, Princeton, NJ 08544, USA.

<sup>5</sup>Current address: National Institute of Biological Sciences, Beijing, 102206, China.

<sup>6</sup>Correspondence should be addressed to D.X. (e-mail: ding.xue@colorado.edu)

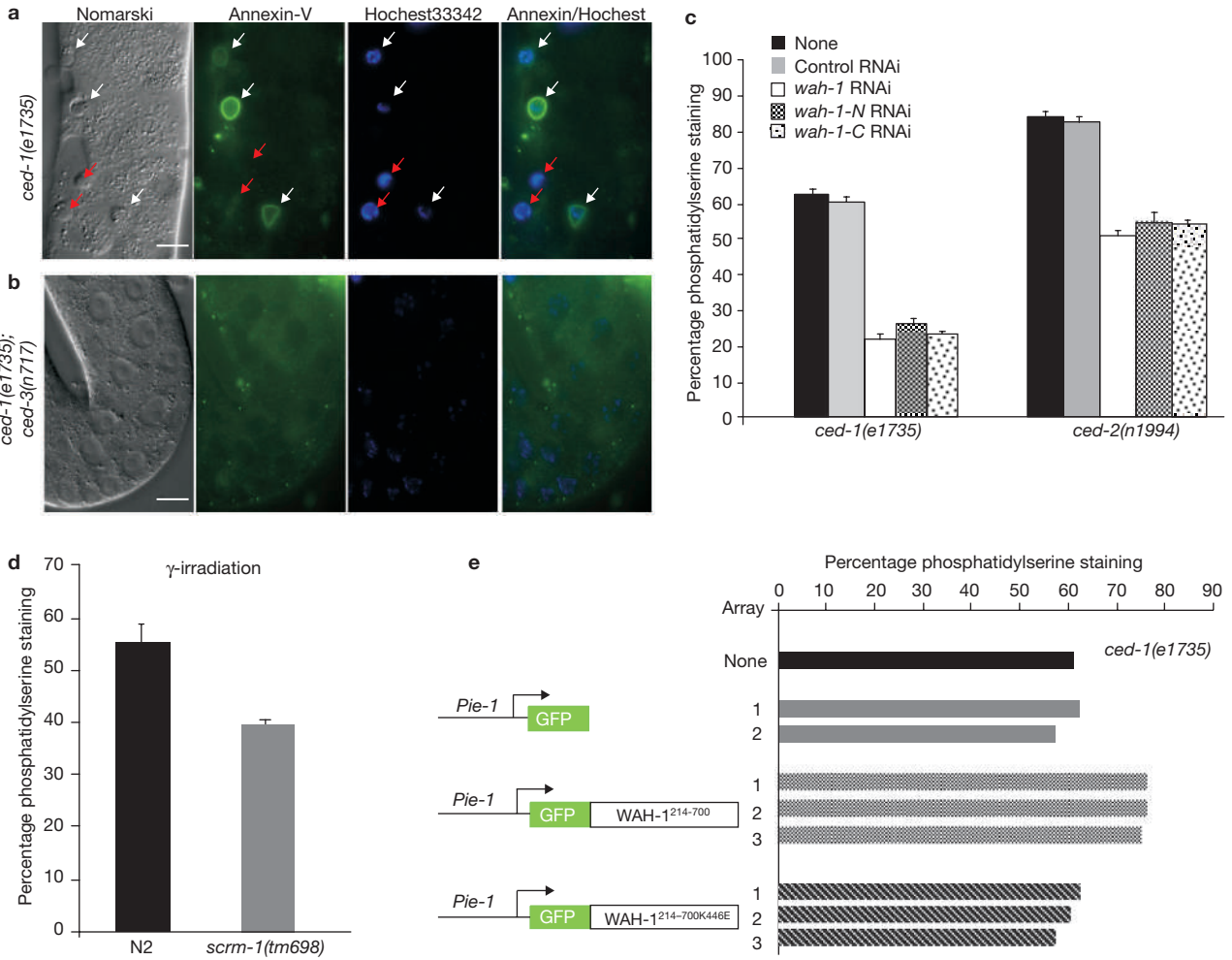


**Figure 1** *wah-1* promotes phosphatidylserine exposure on the surface of apoptotic germ cells. **(a, b)** The exposed gonad of a *ced-1(e1735)* (a) hermaphrodite animal or a *ced-1(e1735); ced-3(n717)* (b) animal was stained with annexin V and Hoechst 33342. Germ-cell corpses were identified by their raised-button-like morphology under the Nomarski optics and the condensed Hoechst 33342 staining pattern. Nomarski, annexin V, Hoechst 33342 and merged images of annexin V and Hoechst 33342 staining of the gonads are shown. Germ-cell corpses stained with both Hoechst and annexin V are indicated by white arrows. Those that were stained by Hoechst but not by annexin V are indicated with red arrows. **(c)** *wah-1* RNAi reduces germ-cell corpse phosphatidylserine staining in *ced-1(e1735)* and *ced-2(n1994)* animals. *wah-1* RNAi experiments were performed using three different RNAi constructs. The *wah-1* RNAi construct contains full-length *wah-1* cDNA sequence. *wah-1-N* RNAi and *wah-1-C* RNAi contain 261 base pair and 360 base pair DNA sequences derived from the amino and carboxy-terminal regions of *wah-1*, respectively. The percentage of phosphatidylserine

staining (y axis) was calculated by dividing the number of germ-cell corpses with phosphatidylserine staining by the number of total germ-cell corpses scored 48 h after the L4 to adult moult. **(d)** Phosphatidylserine exposure in apoptotic germ cells induced by  $\gamma$ -irradiation. Wild-type or *scrm-1(tm698)* animals were aged 24 h after L4 to adult moult before irradiation at 120 Gy. Annexin V staining of apoptotic germ cells was performed and scored 3 h after irradiation. Data shown in **c** and **d** are mean  $\pm$  s.e.m. from three independent experiments. In each experiment, 60–100 germ-cell corpses from 10–16 gonad arms were scored. **(e)** Overexpression of *wah-1* in *C. elegans* germline promotes phosphatidylserine exposure in apoptotic germ cells. The GFP-fusion constructs shown on the left were injected into the *ced-1(e1735)* animals to create complex DNA arrays that facilitate gene expression in the germline. F2 and F3 generations of transgenic animals were used for annexin V staining. Each numbered array represents an independent transgenic line and at least 100 germ-cell corpses from 12–15 gonad arms were scored for each line. The scale bar in **a** represents 6.5  $\mu$ m.

significantly reduced germ-cell corpse phosphatidylserine staining in *ced-2(n1994)* animals. The percentages of germ-cell corpses labelled with annexin V were similar in *ced-1(e1735); wah-1(RNAi)* animals of different adult ages (see Supplementary Information, Table S1) and in animals treated with two additional *wah-1* RNAi constructs (Fig. 1c), *wah-1-N* RNAi and *wah-1-C* RNAi, which contain targeting sequences derived from the amino-terminal and carboxy-terminal regions of *wah-1*, respectively, suggesting that the effect of *wah-1* RNAi on phosphatidylserine exposure is specific and independent of age. These results indicate that the activity of *wah-1* is important for phosphatidylserine externalization in apoptotic germ cells.

We then examined whether *wah-1* can promote phosphatidylserine externalization in *C. elegans* germ cells by overexpressing the active form of WAH-1 (WAH-1<sup>214-700</sup>) under the control of the *pie-1* promoter in an in-frame fusion with GFP (*P<sub>pie-1</sub>*:GFP::WAH-1<sup>214-700</sup>; refs 5, 10). Overexpression of WAH-1<sup>214-700</sup> in germ cells did not increase the number of germ-cell deaths in *ced-1(e1735)* animals (see Supplementary Information, Fig. S1), which is consistent with our previous observation that overexpression of WAH-1<sup>214-700</sup> alone does not cause ectopic somatic cell death in *C. elegans*<sup>5</sup>. However, overexpression of WAH-1<sup>214-700</sup> in germ cells significantly increased the percentage of germ-cell corpses stained with annexin V — 77% of germ-cell corpses from the

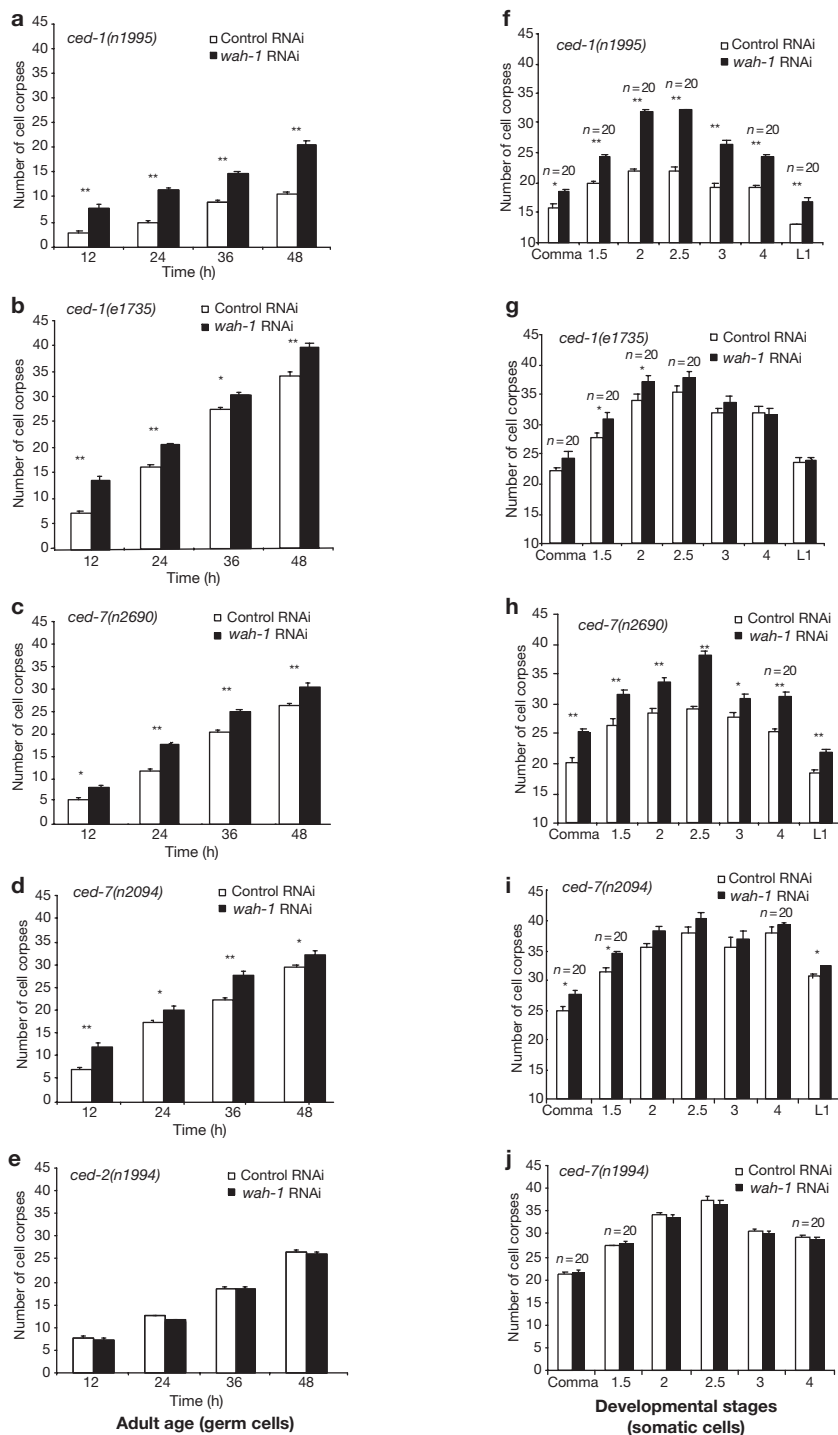


**Figure 2** *wah-1* RNAi affects the clearance of apoptotic cells. (a–j) L1 or L2 larvae from the following animals were treated with *wah-1* RNAi (filled bars) or control RNAi (empty bars) as previously described<sup>5</sup>: *ced-1(n1995)* (a, f), *ced-1(e1735)* (b, g), *ced-7(n2690)* (c, h), *ced-7(n2094)* (d, i) and *ced-2(n1994)* (e, j). The L4 larval stage progeny of the treated animals were transferred to fresh RNAi plates and their progeny were scored for cell corpses. In a–e, the numbers of germ-cell corpses were scored every 12 h after the L4 to adult moult from one gonad arm of the animals. The y axis indicates the average number of germ-cell corpses. The error bars represent s.e.m. Fifteen animals were scored for each time point in a–e. In f–j, the numbers of somatic-cell

corpses were scored at the following embryonic or larval stages: bean or comma (comma), 1.5-fold (1.5), twofold (2), 2.5-fold (2.5), threefold (3), fourfold (4) and early L1 larvae (L1). The y axis indicates the average number of cell corpses counted in the head region of embryos or larvae. The error bars represent s.e.m. Fifteen animals were scored for each developmental stage in f–j unless otherwise indicated. In all panels, data derived from *wah-1* RNAi or control RNAi treatment at multiple time points or developmental stages were compared by two-way analysis of variance. Post hoc comparisons were done by Fisher's protected least squares difference (PLSD). Single asterisks indicate  $P < 0.05$  and double asterisks indicate  $P < 0.0001$ . All other points had  $P$  values  $> 0.05$ .

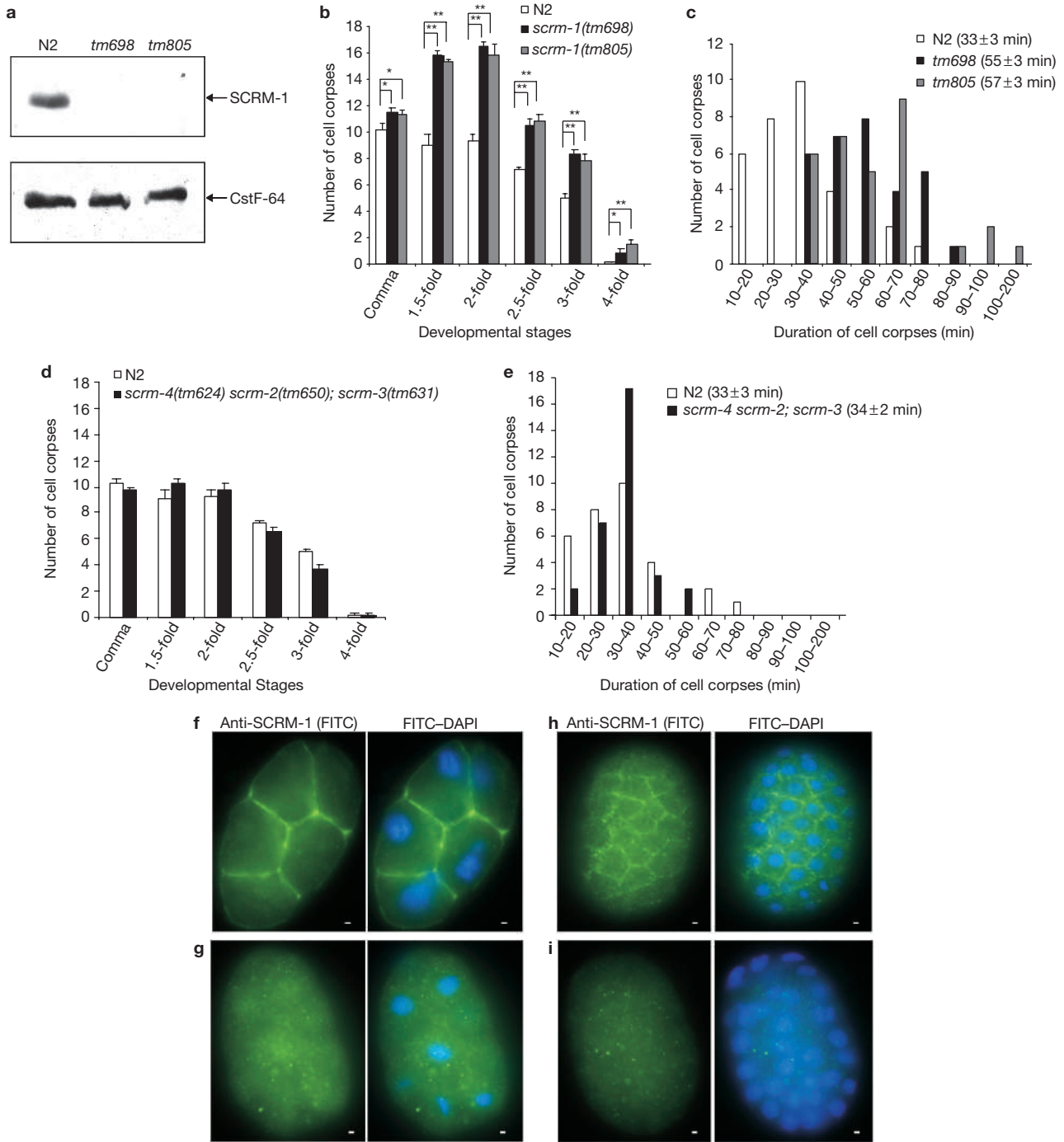


**Figure 3** SCRM-1 is a plasma membrane protein important for cell-corpse engulfment. **(a)** Western blot analysis of the *scrm-1* deletion mutants. *C. elegans* lysates were made from the indicated mix-stage animals and western blot analysis was performed using affinity-purified anti-SCRM-1 antibody. *C. elegans* splicing factor CstF-64 was used as a loading control. **(b–e)** Time-course analysis of embryonic-cell corpses in the *scrm-1* mutants **(b)** or in the *scrm-4 scrm-2; scrm-3* triple mutant **(d)**. Cell corpses were scored at six embryonic stages and analysed statistically as described in Fig. 2. Fifteen animals were scored at each stage. The error bars indicate s.e.m. Single asterisks indicate  $P < 0.05$  and double asterisks indicate  $P < 0.0001$ . All other points had  $P$  values  $> 0.05$ . Four-dimensional microscopy analysis of cell-corpse durations in the *scrm-1*

mutants **(c)** or the *scrm-4 scrm-2; scrm-3* triple mutant **(e)** are also shown. The durations of 31 cell corpses each from N2 embryos ( $n = 4$ , open bars), *scrm-1(tm698)* embryos ( $n = 5$ , black bars), *scrm-1(tm805)* embryos ( $n = 5$ , grey bar) and *scrm* triple-mutant embryos ( $n = 5$ , black bars in **e**) were measured. The numbers in parentheses indicate the average durations of cell corpses ( $\pm$  s.e.m.) from each genotype. The y axis indicates the number of cell corpses within a specific duration range (shown on the x axis). **(f–i)** SCRM-1 localizes to plasma membrane. Images of FITC (SCRM-1 antibody staining) and FITC-DAPI *C. elegans* embryos are shown: a 16-cell stage wild-type **(f)** or *scrm-1(tm805)* **(g)** embryo and a wild-type **(h)** or *scrm-1(tm805)* **(i)** embryo at approximately 200-cell stage. The scale bars indicate 1  $\mu$ m.

*ced-1(e1735)* animals transgenic for the  $P_{pie-1}$ :GFP::WAH-1<sup>214-700</sup> construct were stained (Fig. 1e). In comparison, less than 63% of germ-cell corpses were stained in *ced-1(e1735)* animals carrying either a control transgene ( $P_{pie-1}$ :GFP) or a transgene expressing a mutant WAH-1 protein that fails to activate its effector ( $P_{pie-1}$ :GFP::WAH-1<sup>214-700(K446E)</sup>; see below, Fig. 1e and Supplementary Information, Fig. S2a–c). As overexpression of WAH-1 increases phosphatidylserine externalization, whereas *wah-1* RNAi reduces phosphatidylserine exposure in apoptotic germ cells, *wah-1* may directly activate the phosphatidylserine externalization process in apoptotic cells.

Given that surface-exposed phosphatidylserine can act as an ‘eat-me’ signal to induce phagocytosis<sup>11</sup>, we examined whether *wah-1* affects cell-corpse engulfment in *C. elegans*. *wah-1* RNAi has been shown to delay normal progression of apoptosis, compromise apoptotic DNA degradation and inhibit cell killing in sensitized genetic backgrounds<sup>5</sup>. However, no obvious cell-corpse engulfment defect was detected in *wah-1(RNAi)* animals. To examine this more carefully, animals that were partially defective in cell-corpse engulfment were treated with *wah-1* RNAi and we examined whether *wah-1* RNAi enhanced the engulfment defect in these mutants. Genetic analyses in *C. elegans* have identified several genes that function in two separate pathways to mediate corpse removal in both germ cells and somatic cells, with *ced-1*, *ced-6* and *ced-7* functioning in one pathway and *ced-2*, *ced-5*, *ced-10* and *ced-12* in the other<sup>12</sup>. Double mutants of genes acting in the same pathway have weaker engulfment defects than double mutants of genes acting in different pathways<sup>13</sup>. Interestingly, *wah-1* RNAi strongly enhanced the engulfment defect in *ced-1(n1995)* animals, which contain a partial loss-of-function allele of *ced-1* (ref. 14). In *ced-1(n1995); wah-1(RNAi)* animals, the numbers of persistent germ-cell corpses were significantly higher than those of the *ced-1(n1995); control(RNAi)* animals in four adult stages examined (Fig. 2a). The enhancement of the persistent germ-cell corpse phenotype was weaker in *ced-1(e1735); wah-1(RNAi)* animals (Fig. 2b), which contain a putative null allele of *ced-1* (ref. 14). *wah-1* RNAi similarly enhanced the germ-cell corpse engulfment defect associated with both weak (*n2690*) and strong (*n2094*) alleles of *ced-7* (Fig. 2c, d)<sup>15</sup>, but not that conferred by either weak or strong mutations in the *ced-2*, *ced-5*, *ced-10* and *ced-12* genes (Fig. 2e and data not shown), which function in a different engulfment pathway.

*wah-1* RNAi caused a similar defect in removal of somatic apoptotic cells: it enhanced the somatic cell-corpse engulfment defects associated with both weak and strong *ced-1* and *ced-7* mutations (Fig. 2f–i), but not those of the *ced-2*, *ced-5*, *ced-10* and *ced-12* mutants (Fig. 2j and data not shown). Altogether, these double-mutant analyses clearly indicate that *wah-1* functions in the engulfment pathway mediated by *ced-2*, *ced-5*, *ced-10* and *ced-12* in phagocytes<sup>12</sup> to affect cell corpse clearance, probably through promoting phosphatidylserine externalization in dying cells. Consistent with this model, *wah-1* RNAi did not enhance the engulfment defect of the *psr-1(tm469)* mutant (see Supplementary Information, Fig. S3a), which is defective in PSR-1 — a putative phosphatidylserine-recognizing receptor that functions in the *ced-2*, *ced-5*, *ced-10* and *ced-12* engulfment pathway<sup>16</sup>.

As WAH-1 does not contain any domain or biochemical property that is suggestive of its direct involvement in transbilayer lipid movement<sup>5</sup>, it may function through a lipid-translocating enzyme to promote phosphatidylserine externalization in apoptotic cells. Phospholipid scramblases (PLSCRs), which have been implicated in promoting

ATP-independent, bidirectional lipid scrambling<sup>17–19</sup>, could be potential targets. A BLAST search using the sequences of four human phospholipid scramblases identified eight scramblase homologues in *C. elegans* (see Supplementary Information, Fig. S4a and Supplementary Methods), all of which contain a conserved Ca<sup>2+</sup> binding motif and a putative transmembrane domain<sup>17,20</sup>. They were named *scrm* genes for scramblases. Of the eight SCRM proteins, SCRM-1 is most homologous to four human PLSCRs and thus was characterized first (see Supplementary Information, Fig. S4b).

To investigate the functions of *scrm-1*, two deletion mutations were generated in the *scrm-1* locus (see Supplementary Information, Fig. S4c), *scrm-1(tm698)* and *scrm-1(tm805)*. Both deletions abolished SCRM-1 protein expression in mutant animals based on the western blot analysis using anti-SCRM-1 antibodies (Fig. 3a), and thus are strong loss-of-function or null mutations. In a time-course analysis of embryonic cell corpses, more cell corpses were observed in *scrm-1(tm698)* and *scrm-1(tm805)* embryos than in wild-type embryos (Fig. 3b). The increase in cell corpses in all embryonic stages in the *scrm-1* mutants is likely to be caused by a defect in cell-corpse engulfment, as four-dimensional microscopy analyses of the duration of embryonic cell corpses indicate that cell corpses in both *scrm-1* mutants on average persisted longer than those in wild-type embryos. Specifically, the average cell-corpse duration in *scrm-1(tm698)* and *scrm-1(tm805)* embryos was 55 and 57 min, respectively, compared with 33 min in wild-type embryos (Fig. 3c). These results indicate that the cell-corpse engulfment process is compromised in the *scrm-1* mutants.

We also examined whether *scrm-1* affects phosphatidylserine externalization in apoptotic cells and found that *scrm-1* deletions reduced phosphatidylserine exposure on the surface of germ-cell corpses: for example, 84% of germ-cell corpses were labelled with annexin V in *ced-2(n1994)* animals (Fig. 4a), whereas in *scrm-1(tm698); ced-2(n1994)* and *scrm-1(tm805); ced-2(n1994)* double mutants, only 69 and 67% of germ-cell corpses were stained, displaying 15% and 17% of reductions in staining, respectively. Similar reductions in phosphatidylserine staining were observed in germ-cell corpses in *scrm-1(tm698); ced-5(n1812)* and *scrm-1(tm805); ced-5(n1812)* animals (Fig. 4a), as well as in germ-cell corpses of  $\gamma$ -irradiated *scrm-1(tm698)* animals (Fig. 1d), confirming that the *scrm-1* mutations reduce phosphatidylserine externalization on the surface of apoptotic germ cells.

As both *scrm-1* deletions mutations caused significant, but not strong, defects in cell-corpse engulfment and phosphatidylserine externalization, we examined whether other *C. elegans* SCRM proteins contribute to these two processes. Three deletion mutations (*tm650*, *tm631* and *tm624*) were isolated in three closely related SCRM-1 paralogues (*scrm-2*, *scrm-3* and *scrm-4*; see Supplementary Information, Fig. S4c and Supplementary Methods) and these mutations alone did not cause any defect in cell-corpse engulfment (see Supplementary Information, Fig. S3c) or phosphatidylserine exposure in apoptotic cells (Fig. 4b). Moreover, cell-corpse engulfment seemed normal in a triple mutant of these paralogues, *scrm-4(tm624) scrm-2(tm650); scrm-3(tm631)*, as its embryonic cell-corpse numbers and average duration were indistinguishable from wild-type animals (Fig. 3d, e). Phosphatidylserine staining in the *scrm* triple mutant was only mildly reduced (Fig. 4b). Moreover, treatment of *scrm-4(tm624) scrm-2(tm650); ced-5(n1812); scrm-3(tm631)* animals with *scrm-1* RNAi, which fully phenocopies *scrm-1* deletions in reducing phosphatidylserine exposure

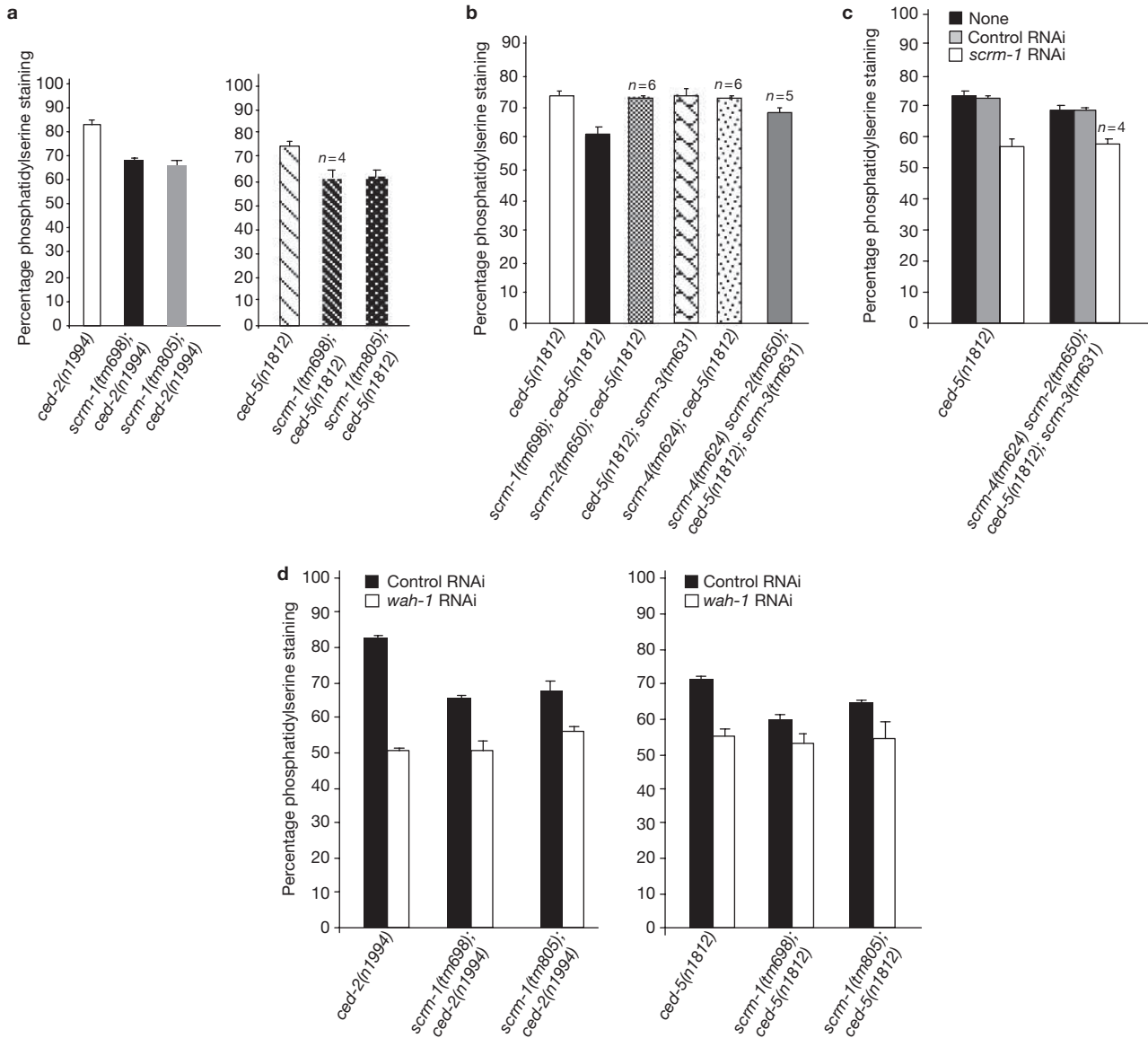


**Figure 4** *scrm-1* and *wah-1* function in the same pathway to promote phosphatidylserine exposure in apoptotic cells. (a–c) *scrm-1* but not *scrm-2*, *scrm-3* or *scrm-4* affects phosphatidylserine exposure in apoptotic germ cells. (d) *scrm-1* and *wah-1* function in the same pathway to promote phosphatidylserine externalization. Phosphatidylserine-staining assays were carried out in various *scrm*; *ced-2* and *scrm*; *ced-5* mutants, or *scrm*; *ced-2* and *scrm*; *ced-5* mutants treated with *scrm-1*

RNAi or *wah-1* RNAi and scored as described in Fig. 1. The genotypes of the animals stained by annexin V are indicated. For each set of experiments, multiple different strains in triplicates were scored blindly for phosphatidylserine staining 48 h after the L4 to adult moult. The error bars indicate s.e.m. Data shown represent three independent experiments unless indicated otherwise. In each experiment at least 60 germ-cell corpses from 10–12 gonadal arms were scored.

in apoptotic cells, did not result in further reduction of phosphatidylserine staining (Fig. 4c), suggesting that *scrm-2*, *scrm-3* and *scrm-4* do not contribute significantly to phosphatidylserine externalization during apoptosis. Individual RNAi treatment of the four remaining *scrm* genes (*scrm-5*, *scrm-6*, *scrm-7* and *scrm-8*) did not produce an obvious defect in phosphatidylserine exposure (see Supplementary Information, Fig. S3d). Thus, of the four worm scramblases that were genetically analyzed, *scrm-1* was the only one that significantly affected phosphatidylserine externalization in apoptotic cells and the cell-corpse engulfment process.

To examine the expression pattern and subcellular localization of SCRM-1 in *C. elegans*, rabbit polyclonal antibodies against SCRM-1 were generated. In western blot analyses, affinity-purified SCRM-1 antibodies specifically recognized a protein band with the predicted

relative molecular mass of SCRM-1 (30,000) in wild-type worm lysate; this band was absent in lysates from both *scrm-1* deletion mutants (Fig. 3a). Wild-type *C. elegans* embryos stained with anti-SCRM-1 antibodies displayed a plasma-membrane staining pattern that was observed in all cells throughout embryogenesis (Fig. 3f, h and data not shown), whereas no specific staining was observed in *scrm-1(tm805)* mutant embryos (Fig. 3g, i). Similar plasma-membrane localization of SCRM-1 was observed in germ cells of wild-type animals, but not in those of *scrm-1(tm805)* animals (see Supplementary Information, Fig. S2d, e). This plasma-membrane localization pattern of SCRM-1 is consistent with its observed role in promoting phosphatidylserine redistribution in the plasma membrane during apoptosis.

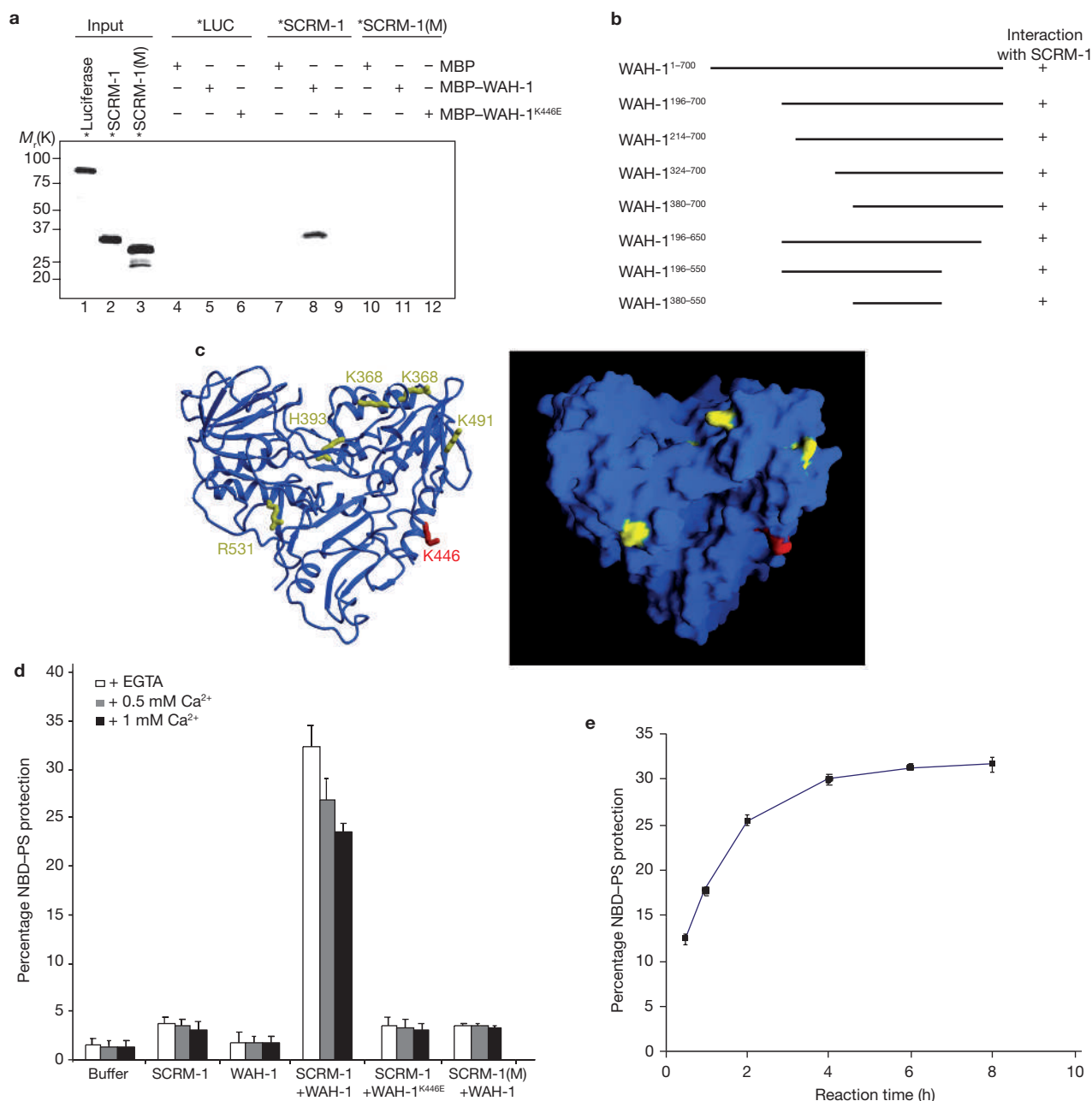


**Figure 5** WAH-1 interacts specifically with SCRMs to activate its phospholipid-scrambling activity. **(a)** WAH-1 associates with SCRMs *in vitro*. Purified MBP, MBP-WAH-1 or MBP-WAH-1<sup>K446E</sup> protein (2.5  $\mu$ g each) immobilized on the amylose resin was incubated with <sup>35</sup>S-methionine-labelled (indicated by asterisk) luciferase (Luc), SCRMs-1 or SCRMs-1(M). The bound proteins were resolved on a 12% SDS-PAGE and detected using a phosphorimager. Lanes 1–3: 5% of the labelled proteins used in the binding reactions. **(b)** WAH-1<sup>380-550</sup> is sufficient to mediate binding to SCRMs-1. Purified GST or GST-SCRMs-1 (2.5  $\mu$ g each) immobilized on glutathione-Sepharose beads was incubated with similar amounts of the full-length or truncated WAH-1 proteins with a six histidine tag. The bound proteins were resolved on SDS-PAGE gels and visualized by western blot analysis using an antibody against the His tag. Interaction between WAH-1 and SCRMs-1 is indicated. **(c)** Structural modelling of WAH-1. The human AIF structure is used to indicate the surface locations of the mutated residues in WAH-1. Residues in human AIF that correspond to the mutated residues in WAH-1 are highlighted in yellow (K386, K388, H393, K491 and R531) and red

(K446). Each residue was substituted with glutamate. Lys 446, but not the other five residues, is critical for the binding of WAH-1 to SCRMs-1. **(d)** WAH-1 activates the phospholipid-scrambling activity of SCRMs-1. Purified SCRMs-1 (6  $\mu$ g) and WAH-1<sup>196-700</sup> (1.25  $\mu$ g), either alone or together, were reconstituted with 250  $\mu$ g liposomes, to which NBD-PS (0.25% in moles) was added after the proteoliposomes were sealed. SCRMs-1(M) + WAH-1, WAH-1<sup>K446E</sup> + SCRMs-1 or a buffer-only control without any protein were similarly reconstituted with liposomes. The proteoliposomes prepared as such were equally divided into six aliquots, supplemented with either 4 mM EGTA or CaCl<sub>2</sub> at the indicated concentration, and incubated at 37 °C in the dark for 6 h. The scramblase activity was measured and presented as percentage NBD-PS protection as described in detail in Methods. **(e)** Time-course analysis of SCRMs-1 phospholipid-scrambling activity. The scramblase activity assays were carried out as described in **d**, except that aliquots were removed and fluorescence was measured at the indicated times. Data shown in **d** and **e** represent three independent experiments, each in duplicates. The error bars indicate s.d.

We next examined whether *wah-1* and *scrm-1* act additively to promote phosphatidylserine exposure in apoptotic cells. *wah-1* RNAi treatment of *scrm-1(tm698)*; *ced-2(n1994)* or *scrm-1(tm805)*; *ced-2(n1994)* animals did not result in further reduction of phosphatidylserine staining in apoptotic germ cells compared with *ced-2(n1994)*; *wah-1(RNAi)* animals (Fig. 4d). Similar results were observed with *wah-1* RNAi treatment of *ced-5* and *scrm-1*; *ced-5* animals (Fig. 4d). These results suggest that *wah-1* and *scrm-1* are likely to function in the same pathway to promote phosphatidylserine externalization.

We then examined whether WAH-1 interacts with SCR-1 *in vitro* using a maltose binding protein (MBP)-fusion protein pulldown assay. *In vitro*-synthesized <sup>35</sup>S-methionine-labelled SCR-1 was pulled down specifically by MBP-WAH-1, but not by MBP alone or by a mutant MBP-WAH-1<sup>K446E</sup> protein (Fig. 5a and see below). In addition, a SCR-1 mutant protein in which all cysteine residues were replaced with alanine did not bind to any of the MBP-WAH-1 or MBP proteins. Moreover, MBP-WAH-1 failed to bind SCR-2, SCR-3 or SCR-4 (see Supplementary Information, Fig. S5a, b), which is consistent with the observations that these three scramblases do not affect phosphatidylserine externalization in worms. Taken together, these results strongly suggest that WAH-1 interacts specifically with SCR-1 *in vitro*.

To identify the region of WAH-1 that is important for binding to SCR-1, the binding of SCR-1 to various WAH-1 truncations was examined and a 170-residue region of WAH-1 (amino acid 380–550) was shown to be sufficient for binding of WAH-1 to SCR-1 (Fig. 5b). The WAH-1 structure was then modelled on the human AIF protein structure<sup>21</sup> and six potential surface residues were identified in this region that may affect the binding of WAH-1 to SCR-1 (Fig. 5c). Substitution of the K446 residue, which locates at a different surface region of WAH-1 from the other five residues (Fig. 5c), specifically abolished the binding of WAH-1 to SCR-1 (Fig. 5a), but did not affect the binding of WAH-1 to DNA (see Supplementary Information, Fig. S5c)<sup>22</sup>. When WAH-1<sup>K446E</sup> was overexpressed in the *C. elegans* germline, it failed to enhance phosphatidylserine externalization in apoptotic germ cells as the wild-type WAH-1 protein did (Fig. 1e and see Supplementary Information, Fig. S2a–c), providing further *in vivo* evidence that the WAH-1–SCR-1 interaction is important for WAH-1 to promote phosphatidylserine exposure in apoptotic cells.

Finally, we examined whether SCR-1 possesses a phospholipid-scrambling activity, and whether WAH-1 affects the activity of SCR-1 using an *in vitro* phospholipid-scrambling assay. Briefly, purified recombinant SCR-1, WAH-1 or both were incorporated into liposomes and fluorescently labelled NBD-PS was used as a probe to measure the phospholipid-scrambling activity of SCR-1. As shown in Fig. 5d, SCR-1 by itself had barely detectable phospholipid-scrambling activity, which was not activated by Ca<sup>2+</sup> at various concentrations tested (data not shown). WAH-1 by itself had no phospholipid-scrambling activity, but could activate the phosphatidylserine-scrambling activity of SCR-1 by tenfold. In contrast, the SCR-1 mutant that did not interact with WAH-1 showed no response to WAH-1 activation and the WAH-1<sup>K446E</sup> mutant that did not bind SCR-1 failed to activate the phosphatidylserine-scrambling activity of SCR-1 (Fig. 5d), indicating that the ability of WAH-1 to bind SCR-1 is crucial for its activation of SCR-1. The activation of SCR-1 by WAH-1 was strongest at a molar ratio of 5:1 (SCR-1:WAH-1), at a pH of approximately 6.75 and at a salt concentration of approximately 50 mM NaCl (see Supplementary Information, Fig. S5d, e and data not shown). A time course analysis revealed that,

under these conditions, the phosphatidylserine-scrambling activity of the SCR-1–WAH-1 complex was detected early in the reaction (12% NBD-PS protection after 30 min), was approximately linear for the first 2 h and reached a plateau at 32% of NBD-PS protection after 4 h (Fig. 5e) — which was estimated to be close to the equilibrium for NBD-PS distribution between the two leaflets of the proteoliposomes (see Methods). The results from these *in vitro* and *in vivo* assays provide strong evidence that WAH-1 can specifically interact with SCR-1 and activate its phospholipid scrambling activity in a Ca<sup>2+</sup>-independent fashion.

How phospholipid asymmetry on the lipid bilayer is generated, maintained and altered (in some biological events such as apoptosis) is a fundamental but poorly understood issue in cell biology<sup>23</sup>. We have developed an *in vivo* phosphatidylserine-staining technique to detect surface-exposed phosphatidylserine in apoptotic cells in *C. elegans* and have used this method, in combination with the genetic and reversed-genetic tools available in *C. elegans*, to dissect the molecular pathway that mediates the phosphatidylserine-externalization process during apoptosis. These studies have led to the identification of a *C. elegans* phospholipid scramblase (SCR-1) as the lipid-translocating enzyme that catalyzes the phosphatidylserine-externalization process and WAH-1, an apoptogenic factor released from mitochondria during apoptosis<sup>5</sup>, as the direct activator of the SCR-1 lipid scramblase, thus establishing a new mitochondria to plasma membrane signalling pathway that promotes cell-surface changes in apoptotic cells. Similar approaches can now be applied to dissect molecular pathways that control the generation and maintenance of phospholipid asymmetry in *C. elegans* and in other organisms. □

## METHODS

**Annexin V staining.** The *C. elegans* gonad is a large cytoplasmic syncytium containing many germ-cell nuclei. The dying germ cells quickly cellularize and pinch off the syncytium very early in the cell-death process<sup>24</sup>. Thus, all apoptotic germ cells are visible on the surface of gonads and are accessible to annexin V staining once gonads are dissected out of the animals. For annexin V staining, gravid hermaphrodite animals were carefully cut open with a surgical blade, at the head or the tail region, on a depression slide in gonad dissection buffer (60 mM NaCl, 32 mM KCl, 3 mM Na<sub>2</sub>HPO<sub>4</sub>, 2 mM MgCl<sub>2</sub>, 20 mM HEPES, 50 µg ml<sup>-1</sup> penicillin, 50 µg ml<sup>-1</sup> streptomycin, 100 µg ml<sup>-1</sup> neomycin, 10 mM Glucose, 33% FCS and 2 mM CaCl<sub>2</sub>) to expose their anterior or posterior gonads from the animal bodies. The dissected animals were then transferred by a mouth pipette to another depression slide with the dissection buffer containing 4 µM Hoechst 33342 and 1 µl Alexa Fluor 488-conjugated annexin V (Molecular Probes, Eugene, OR) for 40 min at 20 °C before they were transferred to a third depression slide containing fresh dissection buffer. The stained animals were then mounted on a slide with a 5% agar pad and examined using a Nomarski microscope equipped with an epifluorescence detector. To score the percentage of germ cell corpses stained by annexin V, the germ-cell corpses were first identified by their raised-button like morphology using Nomarski optics and then the condensed Hoechst 33342 staining using the DAPI filter, before they were examined for annexin V staining.

**Overexpression of WAH-1 in *C. elegans* germ cells.** To express *wah-1* in the germline, a mixture of the following DNA was injected into the *ced-1(e1735)* animals to create complex DNA arrays that facilitate gene expression in the germline<sup>10</sup>: the WAH-1 expression construct linearized with *SacII* (1 µg ml<sup>-1</sup>), the pRF4 (1 µg ml<sup>-1</sup>) construct linearized with *EcoRI* as a dominant coinjection marker and wild-type *C. elegans* genomic DNA digested with *ScaI* (60 µg ml<sup>-1</sup>). F2 and F3 generations of Roller transgenic animals were examined for the expression of GFP before they were stained with annexin V.

**Quantification of cell corpses and extra cells.** The number of somatic-cell corpses in the head region of living embryos or L1 larvae, and the number of germ-cell corpses in one gonad arm from animals at various adult ages were scored using Nomarski optics, as previously described<sup>45,24</sup>.



**Four-dimensional microscopy.** Four-dimensional microscopy analysis of the duration of cell corpses was performed as described previously<sup>16</sup>. For Fig. 3c and e, the durations of four cell divisions in the MS cell lineage from the MS cell to MS.aaaa cell were also followed to ensure that the embryos assayed had similar rates of development. The average duration of four cell divisions in N2 embryos is  $85 \pm 3$  min,  $86 \pm 0.5$  min for *scrm-1(tm698)* embryos,  $87 \pm 0.5$  min for *scrm-1(tm805)* embryos and  $92 \pm 3.9$  min for the *scrm* triple mutant.

**Preparation of liposomes.** Lipids dissolved in chloroform were mixed at a designated composition (phosphatidylcholine, phosphatidylethanolamine, phosphatidylserine, phosphatidylinositol, sphingomyelin and cholesterol at a weight ratio of 42:18.5:2.5:16.5:16)<sup>10</sup> and dried under a stream of nitrogen. The lipids were further dried under vacuum for 1 h followed by suspension in a lipid buffer (1% recrystallized sodium cholate, 1 mM dithiothreitol (DTT) and 10 mM Tris–MES at pH 7.0) to yield a final lipid concentration of 50 mg ml<sup>-1</sup>. The lipid mixture was sonicated in a bath-type sonicator for three 10-min cycles under nitrogen until the lipid preparation became clear. Lipid preparations are then ready for reconstitution with proteins, or can be stored at 4 °C for up to a week. When dialysed or diluted in an assay buffer by twentyfold to reduce the detergent concentration to below 0.05%, the lipid preparation becomes tightly sealed small unilamellar liposomes.

**Reconstitution of SCRM-1 and WAH-1 into proteoliposomes.** Designated amounts of SCRM-1 and WAH-1, alone or together, were mixed in a volume of 10 µl with DTT at a final concentration of 1 mM. Five microlitres of the lipid preparation (250 µg) described above was then added to the protein, or the protein mixture, and mixed thoroughly by vortexing in the presence of 1 mM MgCl<sub>2</sub>. The mixture was incubated at room temperature for 1 h and then 4 °C overnight. The reconstitution mixture was then dialysed in a dialysis disc (Millipore, Billerica, MA; pore size = 0.025 µm) against 3.5 ml assay buffer for 45 min. The default assay buffer contains 50 mM sodium tricine at pH 6.75, 100 mM KCl, 50 mM NaCl and 0.2 mM EGTA. The incorporation of SCRM-1, mutant SCRM-1, WAH-1, or WAH-1<sup>K446E</sup> into liposomes, either alone or together, was examined by 10% SDS–PAGE and Coomassie blue staining and found to be comparable in all experiments (data not shown).

**Phospholipid scramblase assay.** The dialysed proteoliposomes, as described above, were diluted in 0.9 ml assay buffer, followed by addition of NBD–PS (0.25 mol%) and mixed by vortexing. The proteoliposomes were then equally divided into six aliquots: 150 µl each with the addition of either 4 mM EGTA or CaCl<sub>2</sub> at a designated concentration, and incubated at 37 °C in the dark. In the assays to examine the activation of SCRM-1 by WAH-1 (Fig. 5d), sodium dithionite was added to five of the six aliquots to a final concentration of 20 mM to quench the fluorescence of unprotected NBD–PS<sup>11</sup>, and the residual fluorescence was measured (R) in a FLUOstar OPTIMA fluorescence reader. The aliquot without addition of dithionite was measured, which provided a reading of total fluorescence (T). One aliquot served as the background (B), to which 1% NP40 was added in addition to 20 mM dithionite to quench NBD–PS in both membrane leaflets. The phospholipid-scramblase activity was presented as percentage NBD–PS protection, which equals to (R–B)/T. For the time-course analysis of the SCRM-1 activity (Fig. 5e), at each designated time point, 20 mM sodium dithionite was added into the reaction mixture to quench the fluorescence of unprotected NBD–PS, and the residual fluorescence was measured immediately in a FLUOstar OPTIMA fluorescence reader. This procedure for preparing proteoliposomes should yield small unilamellar vesicles (SUV) with an average diameter of 50 nm<sup>25</sup>, of which the surface area of the inner leaflet can be calculated to occupy about 31% of the total surface area of both leaflets. The 32% NBD–PS protection observed after 4 h was estimated to be close to, if not at, the equilibrium for NBD–PS distribution between the inner and outer leaflets of the proteoliposomes. Of note, this *in vitro* phosphatidylserine-scrambling assay may be far from optimal compared with the *in vivo* situation because of differences in the actual lipid compositions and the potential presence of other protein factors.

Note: Supplementary Information is available on the Nature Cell Biology website.

#### ACKNOWLEDGEMENTS

We thank T. Blumenthal for anti-CstF-64 antibody and Geraldine Seydoux for the pTE5 construct. This research was supported by a Burroughs Wellcome

Fund Career Award and a Human Frontier Science Program (HFSP) grant (RGP0016/2005–C) to D.X., a grant from the Ministry of Education, Culture, Sports, Science and Technology of Japan to S.M., and grants from the National Institutes of Health (NIH) to D.X., X.S.X. and Y.S.

#### AUTHOR CONTRIBUTIONS

X.C.W. performed most of the experiments. X.C.W. and D.X. designed and interpreted most of the experiments. J.W. and X.S.W. performed the *in vitro* proteoliposome assays and related data analysis. K.G.A., T.K. and S.M. isolated *scrm* deletion alleles. L.G., Y.G.S., C.L.S., Y.S. and C.L.Y. contributed to the experiments. X.C.W., X.S.X. and D.X. wrote the paper and others commented on the manuscript.

#### COMPETING FINANCIAL INTERESTS

The authors declare that they have no competing financial interests.

Published online at <http://www.nature.com/naturecellbiology/>

Reprints and permissions information is available online at <http://npg.nature.com/reprintsandpermissions/>

- Fadok, V. A. *et al.* Exposure of phosphatidylserine on the surface of apoptotic lymphocytes triggers specific recognition and removal by macrophages. *J. Immunol.* **148**, 2207–2216 (1992).
- Ashman, R. F., Peckham, D., Alhasan, S. & Stunz, L. L. Membrane unpacking and the rapid disposal of apoptotic cells. *Immunol. Lett.* **48**, 159–166 (1995).
- Martin, S. J. *et al.* Early redistribution of plasma membrane phosphatidylserine is a general feature of apoptosis regardless of the initiating stimulus: inhibition by overexpression of *Bcl-2* and *Abl*. *J. Exp. Med.* **182**, 1545–1556 (1995).
- Verhoven, B., Schlegel, R. A. & Williamson, P. Mechanisms of phosphatidylserine exposure, a phagocyte recognition signal, on apoptotic T lymphocytes. *J. Exp. Med.* **182**, 1597–1601 (1995).
- Wang, X., Yang, C., Chai, J., Shi, Y. & Xue, D. Mechanisms of AIF-mediated apoptotic DNA degradation in *Caenorhabditis elegans*. *Science* **298**, 1587–1592 (2002).
- Gumienny, T. L., Lambie, E., Hartwig, E., Horvitz, H. R. & Hengartner, M. O. Genetic control of programmed cell death in the *Caenorhabditis elegans* hermaphrodite germline. *Development* **126**, 1011–1022 (1999).
- Hedgecock, E. M., Sulston, J. E. & Thomson, J. N. Mutations affecting programmed cell deaths in the nematode *Caenorhabditis elegans*. *Science* **220**, 1277–1279 (1983).
- Susin, S. A. *et al.* Molecular characterization of mitochondrial apoptosis-inducing factor. *Nature* **397**, 441–446 (1999).
- Loeffler, M. *et al.* Dominant cell death induction by extramitochondrially targeted apoptosis-inducing factor. *FASEB J.* **15**, 758–767 (2001).
- Tenenhaus, C., Subramaniam, K., Dunn, M. A. & Seydoux, G. PIE-1 is a bifunctional protein that regulates maternal and zygotic gene expression in the embryonic germ line of *Caenorhabditis elegans*. *Genes Dev.* **15**, 1031–1040 (2001).
- Fadok, V. A., Xue, D. & Henson, P. If phosphatidylserine is the death knell, a new phosphatidylserine-specific receptor is the bellringer. *Cell Death Differ.* **8**, 582–587 (2001).
- Reddien, P. W. & Horvitz, H. R. The engulfment process of programmed cell death in *caenorhabditis elegans*. *Annu. Rev. Cell Dev. Biol.* **20**, 193–221 (2004).
- Ellis, R. E., Jacobson, D. M. & Horvitz, H. R. Genes required for the engulfment of cell corpses during programmed cell death in *Caenorhabditis elegans*. *Genetics* **129**, 79–94 (1991).
- Zhou, Z., Hartwig, E. & Horvitz, H. R. CED-1 is a transmembrane receptor that mediates cell corpse engulfment in *C. elegans*. *Cell* **104**, 43–56 (2001).
- Wu, Y. C. & Horvitz, H. R. The *C. elegans* cell corpse engulfment gene *ced-7* encodes a protein similar to ABC transporters. *Cell* **93**, 951–960 (1998).
- Wang, X. *et al.* Cell corpse engulfment mediated by *C. elegans* phosphatidylserine receptor through CED-5 and CED-12. *Science* **302**, 1563–1566 (2003).
- Zhou, Q. *et al.* Molecular cloning of human plasma membrane phospholipid scramblase. A protein mediating transbilayer movement of plasma membrane phospholipids. *J. Biol. Chem.* **272**, 18240–18244 (1997).
- Wiedmer, T., Zhou, Q., Kwok, D. Y. & Sims, P. J. Identification of three new members of the phospholipid scramblase gene family. *Biochim. Biophys. Acta* **1467**, 244–253 (2000).
- Frasch, S. C. *et al.* Regulation of phospholipid scramblase activity during apoptosis and cell activation by protein kinase Cdelta. *J. Biol. Chem.* **275**, 23065–23073 (2000).
- Zhou, Q., Sims, P. J. & Wiedmer, T. Identity of a conserved motif in phospholipid scramblase that is required for Ca<sup>2+</sup>-accelerated transbilayer movement of membrane phospholipids. *Biochemistry* **37**, 2356–2360 (1998).
- Ye, H. *et al.* DNA binding is required for the apoptogenic action of apoptosis inducing factor. *Nature Struct. Biol.* **9**, 680–684 (2002).
- Vahsen, N. *et al.* Physical interaction of apoptosis-inducing factor with DNA and RNA. *Oncogene* **25**, 1763–1774 (2006).
- Balasubramanian, K. & Schroit, A. J. Aminophospholipid asymmetry: A matter of life and death. *Annu. Rev. Physiol.* **65**, 701–734 (2003).
- Gartner, A., Milstein, S., Ahmed, S., Hodgkin, J. & Hengartner, M. O. A conserved checkpoint pathway mediates DNA damage-induced apoptosis and cell cycle arrest in *C. elegans*. *Mol. Cell* **5**, 435–443 (2000).
- Woodlee, M. C. & Papahadjopoulos, D. Liposome preparation and size characterization. *Methods Enzymol.* **171**, 193–217 (1989).